

# Rheo-optics of living polymers: Small-Angle Light Scattering patterns of cetyltrimethylammonium tosylate solutions in presence of sodium bromide

Moisés Romero-Ureña<sup>a</sup>, Luis Medina-Torres<sup>a</sup>, Octavio Manero<sup>b</sup>, J. Esteban López-Aguilar<sup>a,\*</sup>

<sup>a</sup>) Facultad de Química, Departamento de Ingeniería Química, Universidad Nacional Autónoma de México (UNAM), Ciudad Universitaria, Coyoacán, Ciudad de México, 04510, México; <sup>b</sup>) Instituto de Investigaciones en Materiales, UNAM, Apto. Postal 70-360, Ciudad de México, 04510, México; \*Corresponding author email: jelopezaguilar@quimica.unam.mx

**Abstract:** In this work, we present a rheo-optical study based on Small-Angle Light Scattering (SALS) patterns of the simple shear-flow response of cetyltrimethylammonium tosylate solutions (CTAT; 0.12 M), in the presence of sodium bromide (NaBr) at different concentrations  $[NaBr] = \{0, 0.12, 0.19, 0.25, 0.3\}$  M. Here, evidence is provided on a relationship between the rheological and light scattering data that reveals a transition into a fast-breaking regime in the dynamics of CTAT/NaBr wormlike micellar solutions (WLM). This transition is exposed and provoked through increasing NaBr concentration, and apparent through: (i) a decrease in the relaxation time  $\lambda_0$ , along with (ii) a decrement of the low-shear-rate viscosity  $\eta_0$ ; (iii) the formation of butterfly-like scattering patterns, caused by concentration fluctuations due to the imposed flow, correlated with (iv) the development of banded flows in the velocity-gradient direction, and (v) signs of a transition to a distinct flow regime, recorded through the formation of a second peak in the structure factor. In addition, we report the Cox-Merz rule fulfilment at molar salt-to-surfactant ratios of  $R \geq 1.5$ , which, according to estimates of the BMP model, results in structure-recovery time-scales shorter than the flow characteristic-time. Finally, from a theoretical perspective, BMP-model predictions are provided for the shear-stress and the first normal-stress growth coefficient in transient start-up simple shear flow for the samples with  $R=0$  and  $R=1.5$ , for which signs of non-linear behaviour are recorded through oscillatory signals.

**Introduction.** Worm-like micellar (WLM) solutions have been studied in recent years due to their different technological applications, such as fracturing fluids in oil fields; friction-reducing agents in urban heating systems and home-cleaning products.<sup>1</sup> WLM solutions can be formed with different surfactants, for which cationic, anionic, or mixes of both can be employed for their assembly.<sup>2,3</sup> It is well known that the rheological properties of these viscoelastic solutions are influenced by surfactant concentration, temperature, pH, and salinity.<sup>2-10</sup> In the case of cationic-surfactant-based WLM solutions, the influence of simple salts and hydrotopes has been studied extensively.<sup>7-12</sup> Several research works have reported the influence of ionic strength on WLM solution linear and non-linear rheological properties.<sup>11,12</sup> Even some studies reported that their rheological properties follow trends marked by the Hofmeister series.<sup>7,11,12</sup>

The counterions added to WLM solutions also play a role in their optical properties.<sup>4,8,10</sup> It has been reported that the salt-concentration increase promotes light scattering, with high salt-concentration triggering an evolution in the scattering patterns from “butterfly-like” to “tulip-like” at high shear rates.<sup>10</sup> For aqueous solutions of CTAT-NaCl, some authors<sup>8</sup> demonstrated that, contrary to CTAB/NaSal<sup>10</sup> solutions, the CTAT-NaCl<sup>8</sup> system do not reach the pattern-formation evolution as reported by Kadoma & Egmond.<sup>10</sup> In this work, we study the rheological response of a non-conventional CTAT-NaBr micellar system and expose its fast-breaking regime in terms of typical rheological tests on steady simple shear and oscillatory flow, complemented with data captured through small-angle light scattering (SALS).

## Experiments

**Sample preparation.** The WLM system studied in this work is a solution of

cetyltrimethylammonium tosylate (CTAT, 455.74 g/mol) at 0.12 M and sodium bromide (NaBr, 102.89 g/mol), varying the NaBr concentration as listed in Table 1. Samples were prepared by dissolving the prescribed amounts of NaBr and CTAT into distilled water. Before carrying out the experiments, the samples were subjected to sonic agitation for about 1 to 2 h at a temperature of 30 °C.

**Table 1.** Solutions of CTAT/NaBr analysed.

CTAT [M]	NaBr [M]	R=[NaBr]/[CTAT]
0.12	0	0
0.12	0.12	1
0.12	0.2	1.5
0.12	0.25	1.96
0.12	0.3	2.38

**Simple shearing flows.** Steady simple shear and oscillatory flow measurements were performed using a TA Instruments DHR 3 rheometer coupled to a SALS fixture. A parallel-plate geometry was used (translucent upper plate quartz fixture) with the gap-size of 0.9 mm. A  $\dot{\gamma} = 0.01 \text{ s}^{-1}$  pre-shear was imposed on each sample for 100 s. The steady simple-shear flow and oscillatory flow experiments were performed in a range of  $0.01 \leq \dot{\gamma} \leq 100$  and  $0.01 \leq \omega \leq 300 \text{ rad}\cdot\text{s}^{-1}$ , respectively. All experiments were carried out at 30 °C.

**SALS measurements.** The lower plate of the fixture has a sapphire window where the laser is located. The laser is composed of a Class II 0.95 mW diode, with a beam of 635 nm wavelength and a diameter of 1.1 mm. For further details, see Romero-Ureña et al.<sup>16</sup>

**Results y discussion.** SAOS and steady simple shear flows are analysed in terms of experimental trends towards the Cox–Merz rule and the evolution of the SALS patterns, and their correlation with the CTAT–NaBr WLM solution rheological response towards the fast-breaking of fluid re-structuration. In addition, a prediction in simple shear start-up flow of our WLM solutions is provided using the BMP model.

**Small-amplitude oscillatory shear flow.** At low frequencies, the behaviour of the CTAT/NaBr WLM solutions is Maxwellian. This response changes as the samples are subjected to higher frequencies. Here, an increase in the Br<sup>-</sup> ion concentration causes a

shift to lower values of relaxation-time  $\lambda_0$ , which implies a change in the WLM solution viscoelastic characteristics (see Table 2 and Fig. 1).

SAOS results were analysed following the Cates model for living polymers.<sup>8,13</sup> The Cates model establishes a relationship between two characteristic times,  $\zeta = \tau_{\text{break}}/\tau_{\text{rep}}$ , where  $\tau_{\text{break}}$  is the breakage time and  $\tau_{\text{rep}}$  is reptation time. The Cates ratio has two limits: (i) a fast-breaking limit with  $\tau_{\text{break}} < \tau_{\text{rep}}$ ; and (ii) a slow-breaking limit with  $\tau_{\text{break}} \sim \tau_{\text{rep}}$ .<sup>8</sup> For our samples,  $\zeta < 1$ , which implies a fast-breaking regime limit in our samples (see Table 2). In addition, using the Cates model,<sup>13</sup> one can estimate the mesoscopic wormlike micelle length-scales,<sup>2,8</sup> as given by Eq. (1):

$$\frac{G''_{\min}}{G_0} = A \frac{l_e}{L_c}, \quad (1)$$

here,  $G_0$  is the elastic modulus at high frequencies,  $A$  is a dimensionless parameter to be determined,  $l_e$  is the micelle entanglement length,  $L_c$  is the average length of the micelles, and  $G''_{\min}$  is defined as:

$$G''_{\min} = 2 * G_0(\lambda_{\infty}/\lambda_0)^{1/2}, \quad (2)$$

where  $\lambda_{\infty}$  is the relaxation-time measured at high shear-rates. Here, In Table 2, one may note that  $L_c$  decreases with NaBr concentration, witnessing the effects of adding the salt to the CTAT solution and changing the viscoelastic response of the samples.

**Table 2.** Solutions of CTAT/NaBr analysed.

R	$G_0$ [Pa]	$\lambda_0$ [s]	$\tau_{\text{break}}$ [s]	$\zeta$	$L_c$ [μm]
0	305	0.502	0.090	0.031	4.86
1	280	0.243	0.450	0.035	4.49
1.5	236	0.241	0.050	0.043	4.01
1.96	220	0.253	0.055	0.048	3.70
2.38	240	0.256	0.054	0.044	3.89

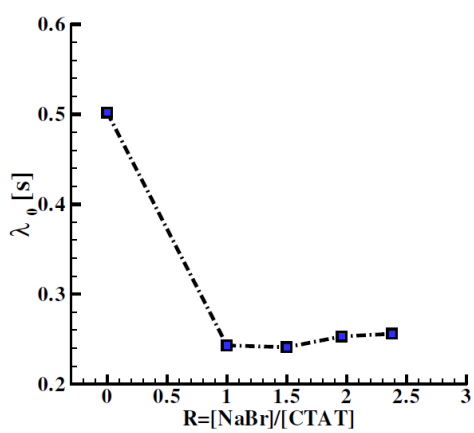


Figure 1.  $\lambda_0$  against salt-to-surfactant molar ratio (R).

**Steady simple shear flow.** Results under steady simple shear flow are illustrated in Fig. 2. Consistently with the findings under SAOS, a decrease in viscosity is observed at low shear rates for the samples containing NaBr<sup>7,8,10,14</sup>. This may be due to a structure transition in which micelles form transient connection points that can slide along the micelle back-bone, which reflect macroscopically in the viscosity decrease of the solution.<sup>8,10</sup>

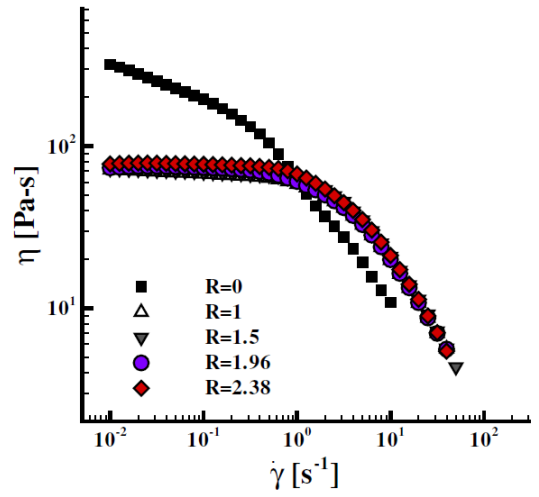


Figure 2.  $\eta$  against  $\dot{\gamma}$  for  $R = \{0, 1, 1.5, 1.96, 2.38\}$ .

**The Cox-Merz rule.** Fig. 3 shows that the increase in NaBr concentration causes a gradual approximation between both  $\eta$  and  $\eta^*$  viscosities. It has been explained<sup>15</sup> that, for WLM solutions, the deviation from the Cox-Merz rule is due to a difference between the structural relaxation time  $\lambda_s$  and the Maxwell relaxation time at high shear-rates  $\lambda_\infty$ . Hence,

under  $\lambda_s/\lambda_\infty=1$ ,  $\eta$  and  $\eta^*$  will be equal. According to this, the NaBr-addition promotes a transition to a fast-breaking regime dynamics, feature that is accompanied by converging  $\eta$  and  $\eta^*$ , characteristic of the Cox-Merz rule.<sup>7,8,15</sup> Our results with the CTAT/NaBr system follow the same trend as the CTAT/NaCl system.<sup>8</sup> In the CTAT/NaCl case, the Cox-Merz rule is fulfilled at the relatively lower R-ratios of  $R \geq 0.25$ ,<sup>8</sup> whilst, contrastingly, in the CTAT/NaBr case, such feature happens at  $R \geq 1.5$ .<sup>16</sup>

**SALS patterns.** The scattering patterns presented in Fig. 4 reflect the coupling of concentration fluctuations with the imposed flow, where one observes patterns in the form of *butterfly wings* located along the flow-direction with increasing R and shear-rate, and which are associated with an increase in concentration fluctuations in the shear-thinning regime. To complement the rheo-optical data, Fig. 5 display plots of the dimensionless structure-factor intensity ( $S/S_0$ ) against the normalised scattering vector ( $q/q^*$ ), for which a rise in the shear-rate applied provokes a stronger intensity of  $S/S_0$ ,<sup>16</sup> corresponding to the enlargement of the butterfly wing apparent in the scattering patterns and accompanied in Fig. 5a with the appearance of a second peak in the structure factor at relatively larger dispersion vector intensities.

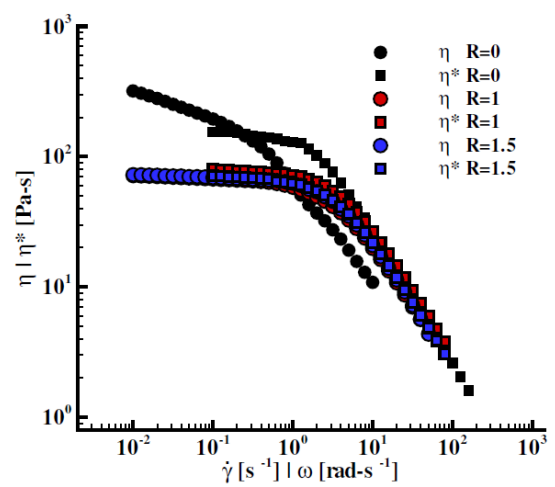
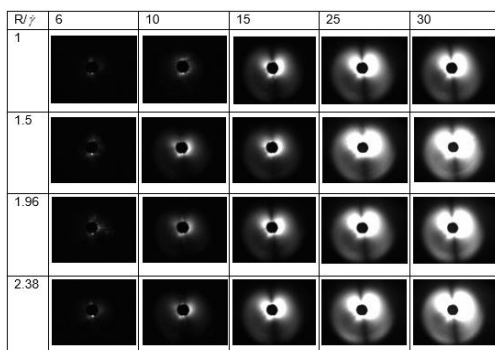


Figure 3.  $\eta$  against  $\dot{\gamma}$  and  $\eta^*$  against  $\omega$  for  $R = \{0, 1, 1.5\}$



**Figure 4.** Scattering patterns of the CTAT/NaBr samples against  $\dot{\gamma}$  and molar salt-to-surfactant ratio  $R$ ;  $\dot{\gamma} = \{6, 10, 15, 25, 30\}$  and  $R = \{1, 1.5, 1.96, 2.38\}$ .

**Instabilities in CTAT/NaBr wormlike micellar solutions under simple shearing flows.** The predictions in simple shear start-up flow of the CTAT/NaBr WLM solutions with the BMP model<sup>8,15</sup> is illustrated in Fig. 6 and the BMP-model parameters obtained are listed in Table 3.<sup>16</sup> The BMP model is defined as:

$$\boldsymbol{\tau} = \boldsymbol{\tau}_p + \boldsymbol{\tau}_s, \quad (3)$$

$$f\boldsymbol{\tau}_p + \lambda_1 \dot{\boldsymbol{\tau}}_p = 2\eta_{p0} \mathbf{D}, \quad (4)$$

$$\frac{\partial f}{\partial t} = \frac{1}{\lambda_s} (1-f) + k_0 (1 + \zeta II_D) \left( \frac{\eta_{p0}}{\eta_\infty} - f \right) |\boldsymbol{\tau}_p : \mathbf{D}|. \quad (5)$$

Eq.(3) represents the total stress resulting from the sum of the micellar solute ( $\boldsymbol{\tau}_s$ ) and solvent stress of Newtonian nature. The solute stress  $\boldsymbol{\tau}_p$  (Eq. 4) follows a Maxwell constitutive equation under the upper-convected stress time-variation  $\dot{\boldsymbol{\tau}}_p = \frac{\partial \boldsymbol{\tau}_p}{\partial t} + \mathbf{v} \cdot \nabla \boldsymbol{\tau}_p - \nabla \mathbf{v}^T \cdot \boldsymbol{\tau}_p - \boldsymbol{\tau}_p \cdot \nabla \mathbf{v}$ , coupled to an evolution equation (Eq. 5) that states the dynamics of micellar breakage and reformation. Here,  $f$  is a measure to estimate the internal-structure is the WLM solutions;  $\eta_0$  and  $\eta_\infty$  are the first and second Newtonian viscosity-plateaux, respectively;  $\eta_s$  is the solvent viscosity;  $\lambda_1$  and  $\lambda_s$  are the relaxation and construction-destruction time, respectively.  $k_0$  is the inverse of the characteristic stress for micellar destruction, and  $\zeta$  is the shear-banding intensity parameter.

**Table 3.** BMP model fitting parameters for CTAT solutions.

R	$\kappa_0$ [Pa <sup>-1</sup> ]	$\lambda_s$ [s]	$\zeta$ [s]	$\eta_\infty$	$\lambda_s/\lambda_\infty$
0	0.001	0.001	0.00	0.01	28.57
1	0.0009	0.019	0.01	0.85	6.39
1.5	0.0012	0.021	0.03	1.8	2.69
1.96	0.002	0.022	0.03	2.5	1.87
2.38	0.005	0.020	0.04	4.1	1.25

To evidence the role played by the micellar fast-breaking dynamics in the development of flow instabilities, a predictive study is performed using the BMP model on steady simple shear stress and first normal-stress growth coefficient in transient test. In Fig. 6, one may note that  $R$ -increase promotes the development of relatively-slow transients appearing as oscillations in time towards a steady-state value, in contrast to the NaBr-free sample, for which such transients appear depressed. These results agree with experimental reports on instabilities observed in WLM solutions under banding and non-banding conditions.<sup>7,15-18</sup>

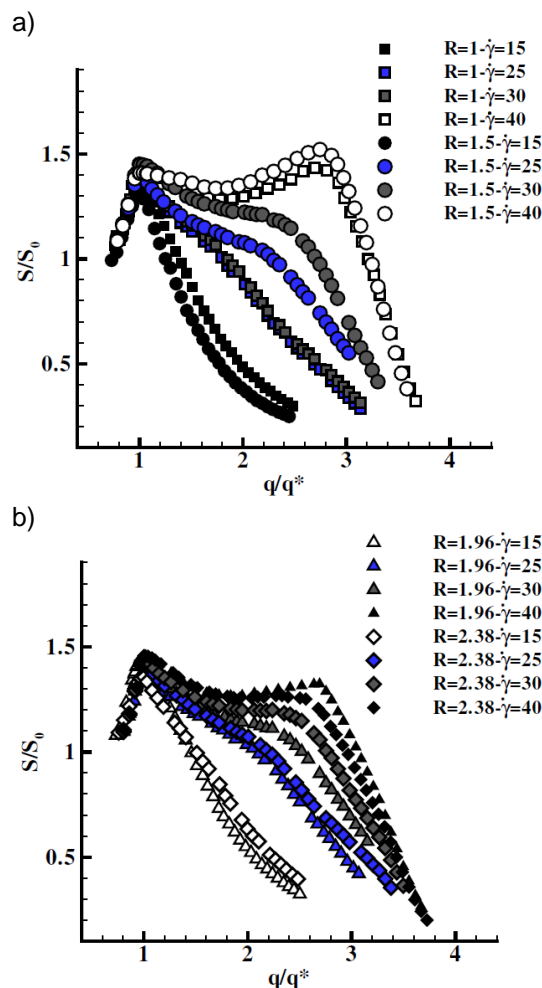


**Figure 5.**  $S/S_0$  against  $q/q^*$  for: (a)  $R = \{1, 1.5\}$  and (b)  $R = \{1.96, 2.38\}$ . Both at  $\dot{\gamma} = \{15, 25, 30, 40\}$ .

**Conclusions.** We have found direct experimental and theoretical evidence on the description of such micellar fast-breaking dynamics and the relationship of this regime

with a series of flow features and responses for our CTAT/NaBr WLM solutions. Experimentally, we found:

(i) *Butterfly-like light-scattering pattern formation.* We found that for the CTAT-NaBr system, a  $\dot{\gamma} = 10 \text{ s}^{-1}$  and salt-to-surfactant ratio of  $R \geq 1$  are required to develop butterfly-shaped patterns, whilst for the CTAT-NaCl system,<sup>8</sup> these conditions are less stringent, i.e.  $\dot{\gamma} = 6 \text{ s}^{-1}$  and  $R \geq 0.16$ .

(ii) *Cox–Merz rule fulfilment.* The comparison of the viscosities in steady simple-shear flow and oscillatory flow show agreement with the Cox–Merz rule, which occurs at  $R \geq 1.5$  for the CTAT-NaBr<sup>16</sup> case, whilst for the CTAT-NaCl system, this rule is fulfilled at  $R \geq 0.25$ , following the ionic strength classification provided by the Hofmeister series.<sup>7,8</sup>

Theoretically, we found:

(i) *Ratio of the micellar construction time  $\lambda_s$  to the viscoelastic characteristic time at high shear-rate  $\lambda_\infty$ .* We found that  $\lambda_s/\lambda_\infty$  (see Table. 3) tends to unity under the fast-breaking regime ( $R \geq 1$ ) for the CTAT-NaBr.<sup>16</sup> This result concurs with findings for CTAT-NaCl WLM solutions.<sup>8</sup>

(ii) *Shear banding.* Our CTAT/NaBr solutions<sup>16</sup> displayed non-monotonic flow curves, characteristic of shear-banding fluids<sup>17,18</sup> characterised with the BMP model.<sup>8,14-16</sup> Our theoretical and experimental results indicate the presence of shear bands, linked with transient overshoot responses in stress (see next point).

(iii) *Non-linear transients in start-up shearing flows.* BMP-model predictions are provided for the start-up shearing flow of two specific samples (one salt-free and another with  $R = 1.5$  salt-to-surfactant molar ratio). The  $R = 1.5$  sample displays pronounced transients in stress signals.<sup>7,8,10,14-18</sup> In contrast, a salt-free CTAT solution, displays a linear exponential trend.

### Acknowledgements.

JEL-A acknowledges the support from Consejo Nacional de Ciencias, Humanidades y Tecnologías (CONAHCYT, Mexico - grant number CF-2023-I-318) and from Universidad Nacional Autónoma de México UNAM (grant numbers PAPIIT IN106424 and PAIP 5000-

9172 Facultad de Química). JEL-A and OM acknowledge the support from UNAM under the project with Grant No. PAPIIT IN100623. MR-U acknowledges the support from Consejo Nacional de Ciencias, Humanidades y Tecnologías (CONAHCYT, Mexico) for the scholarship (CVU number 1084375) to fund his post-graduate studies.

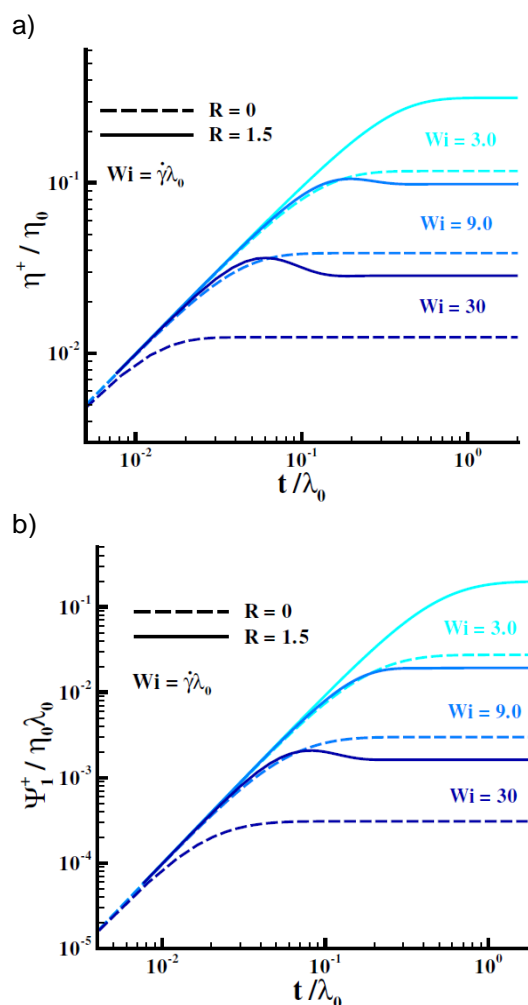


**Figure 6.** BMP model predictions in simple shear start-up flow for: (a) dimensionless shear-stress growth coefficient; (b) dimensionless first normal-stress growth coefficient.

### References.

- (1) Yang, J. Viscoelastic wormlike micelles and their applications, *Curr. Opin. Colloid Interface Sci.* 7 (5–6) (2002) 276–281.
- (2) Dreiss, C. A. Wormlike micelles: where do we stand? Recent developments, linear rheology and scattering techniques, *Soft Matter* 3 (8) (2007) 956–970.

- (3) Berret, J. F. Rheology of wormlike micelles: Equilibrium properties and shear banding transitions, in: *Molecular Gels: Materials with Self-Assembled Fibrillar Networks*, Springer, 2006, pp. 667–720.
- (4) Schubert, B. A.; Kaler, E. W.; Wagner, N.J. The microstructure and rheology of mixed cationic/anionic wormlike micelles, *Langmuir* 19 (10) (2003) 4079–4089.
- (5) Rojas M. R.; Müller, A. J.; Sáez, A. E. Effect of ionic environment on the rheology of wormlike micelle solutions of mixtures of surfactants with opposite charge, *J. Colloid Interface Sci.* 342 (1) (2010) 103–109.
- (6) Dai, C.; Yan, Z.; You, Q.; Du, M.; Zhao, M. Formation of worm-like micelles in mixed N-hexadecyl-N-methylpyrrolidinium bromide-based cationic surfactant and anionic surfactant systems, *PLoS One* 9 (7) (2014) e102539.
- (7) Macías, E.; Bautista, F.; Pérez-López, J.; Schulz, P.; Gradzielski, M.; Manero, O.; Puig, J.; Escalante, J. Effect of ionic strength on rheological behavior of polymerlike cetyltrimethylammonium tosylate micellar solutions, *Soft Matter* 7 (5) (2011) 2094–2102.
- (8) Fierro, C.; Medina-Torres, L.; Bautista, F.; Herrera-Valencia, E. E.; Calderas, F.; Manero, O. The structure factor in flowing wormlike micellar solutions, *J. Non-Newton. Fluid Mech.* 289 (2021) 104469.
- (9) Gouveia, L. M.; Müller, A. J. The effect of NaCl addition on the rheological behavior of cetyltrimethylammonium p-toluenesulfonate (CTAT) aqueous solutions and their mixtures with hydrophobically modified polyacrylamide aqueous solutions, *Rheol. Acta* 48 (2009) 163–175.
- (10) Kadoma, I. A.; van Egmond, J. W.; Shear-enhanced orientation and concentration fluctuations in wormlike micelles: Effect of salt, *Langmuir* 13 (17) (1997) 4551–4561.
- (11) Gaudino, D.; Pasquino, R.; Grizzuti, N.; Adding salt to a surfactant solution: Linear rheological response of the resulting morphologies, *J. Rheol.* 59 (6) (2015) 1363–1375.
- (12) Alkschbirs, M.; Percebom, A. M.; Loh, W.; Westfahl, H. Jr.; Cardoso, M.B.; Sabadini, E. Effects of some anions of the Hofmeister series on the rheology of cetyltrimethylammonium-salicylate wormlike micelles, *Colloids Surf. A Physicochem. Eng. Asp.* 470 (2015) 1–7.
- (13) Cates, M. E. Reptation of living polymers: dynamics of entangled polymers in the presence of reversible chain-scission reactions, *Macromolecules* 20 (9) (1987) 2289–2296.
- (14) Soltero, J.; Bautista, F.; Puig, J.; Manero O. Rheology of cetyltrimethylammonium P-toluenesulfonate- water system. 3. nonlinear viscoelasticity, *Langmuir* 15 (5) (1999) 1604–1612.
- (15) Manero, O.; Bautista, F.; Soltero, J. F. A.; Puig, J.E. Dynamics of worm-like micelles: the Cox–Merz rule, *J. Non-Newton. Fluid Mech.* 106 (1) (2002) 1–15.
- (16) Romero-Ureña, M.; Medina-Torres, L.; Manero, O.; López-Aguilar, J. E. Rheo-optics of giant micelles: SALS patterns of cetyltrimethylammonium tosylate solutions in presence of sodium bromide, *J. Non-Newton. Fluid Mech.* (2024) 105286.
- (17) Lerouge, S.; Berret, J. F. Shear-induced transitions and instabilities in surfactant wormlike micelles, *Adv. Polym. Sci.* (2010) 1–71.
- (18) Hu, Y. T.; Lips, A. Kinetics and mechanism of shear banding in an entangled micellar solution, *J. Rheol.* 49 (5) (2005) 1001–1027.